

**UCC Library and UCC researchers have made this item openly available.  
Please [let us know](#) how this has helped you. Thanks!**

<b>Title</b>	Vapor-phase passivation of chlorine-terminated Ge(100) using self-assembled monolayers of hexanethiol
<b>Author(s)</b>	Garvey, Shane; Holmes, Justin D.; Kim, Y. S.; Long, Brenda
<b>Publication date</b>	2020-06-05
<b>Original citation</b>	Garvey, S., Holmes, J. D., Kim, Y. S., and Long, B. (2020) 'Vapor-phase passivation of chlorine-terminated Ge(100) using self-assembled monolayers of hexanethiol', ACS Applied Materials & Interfaces, 12(26), pp. 29899-29907. doi: 10.1021/acsami.0c02548/acs.jpcc.0c04034
<b>Type of publication</b>	Article (peer-reviewed)
<b>Link to publisher's version</b>	<a href="http://dx.doi.org/10.1021/acsami.0c02548">http://dx.doi.org/10.1021/acsami.0c02548</a> Access to the full text of the published version may require a subscription.
<b>Rights</b>	© 2020, American Chemical Society. This document is the Accepted Manuscript version of a Published Work that appeared in final form in ACS Applied Materials and Interfaces after technical editing by the publisher. To access the final edited and published work see <a href="https://pubs.acs.org/doi/10.1021/acsami.0c02548">https://pubs.acs.org/doi/10.1021/acsami.0c02548</a>
<b>Embargo information</b>	Access to this article is restricted until 12 months after publication by request of the publisher.
<b>Embargo lift date</b>	2021-06-05
<b>Item downloaded from</b>	<a href="http://hdl.handle.net/10468/10304">http://hdl.handle.net/10468/10304</a>

Downloaded on 2021-11-29T00:15:40Z

## Vapor-phase passivation of chlorine-terminated Ge(100) using self-assembled monolayers of hexanethiol

Shane Garvey, Justin D. Holmes, YS Kim, and Brenda Long

*ACS Appl. Mater. Interfaces*, **Just Accepted Manuscript** • DOI:  
10.1021/acsami.0c02548 • Publication Date (Web): 05 Jun 2020

Downloaded from [pubs.acs.org](https://pubs.acs.org) on June 16, 2020

### Just Accepted

“Just Accepted” manuscripts have been peer-reviewed and accepted for publication. They are posted online prior to technical editing, formatting for publication and author proofing. The American Chemical Society provides “Just Accepted” as a service to the research community to expedite the dissemination of scientific material as soon as possible after acceptance. “Just Accepted” manuscripts appear in full in PDF format accompanied by an HTML abstract. “Just Accepted” manuscripts have been fully peer reviewed, but should not be considered the official version of record. They are citable by the Digital Object Identifier (DOI®). “Just Accepted” is an optional service offered to authors. Therefore, the “Just Accepted” Web site may not include all articles that will be published in the journal. After a manuscript is technically edited and formatted, it will be removed from the “Just Accepted” Web site and published as an ASAP article. Note that technical editing may introduce minor changes to the manuscript text and/or graphics which could affect content, and all legal disclaimers and ethical guidelines that apply to the journal pertain. ACS cannot be held responsible for errors or consequences arising from the use of information contained in these “Just Accepted” manuscripts.

1  
2  
3  
4  
5  
6  
7 1 Vapor-phase passivation of chlorine-  
8  
9  
10  
11 2 terminated Ge(100) using self-assembled  
12  
13  
14  
15 3 monolayers of hexanethiol  
16  
17  
18  
19

20 4 Shane Garvey,<sup>†‡</sup> Justin D. Holmes,<sup>†</sup> YS Kim,<sup>§</sup> and Brenda Long<sup>†\*</sup>  
21  
22

23  
24 † School of Chemistry & AMBER Centre, University College Cork, Cork,  
25  
26 T12 YN60, Ireland.  
27  
28

29  
30 ‡ Tyndall National Institute, University College Cork, Cork, T12 R5CP,  
31  
32 Ireland.  
33  
34

35 9 § Lam Research Corp., Fremont, CA 94538, USA.  
36  
37

38  
39 10 **Keywords:**  
40  
41  
42  
43  
44  
45  
46  
47  
48

1  
2  
3 11 Germanium, Passivation, Self-Assembled Monolayers, Oxidation, X-ray  
4  
5 12 Photoelectron Spectroscopy, Thiols.  
6  
7

8  
9 13 Corresponding Author: [brenda.long@ucc.ie](mailto:brenda.long@ucc.ie)  
10

11  
12  
13 14 **Abstract:**  
14  
15

16 15 Continued scaling of electronic devices shows the need to incorporate high  
17  
18 16 mobility alternatives to silicon, the cornerstone of the semiconductor  
19  
20 17 industry, into modern field effect transistor (FET) devices. Germanium is  
21  
22 18 well poised to serve as the channel material in FET devices as it boasts an  
23  
24 19 electron and hole mobility more than twice and four times that of Si,  
25  
26 20 respectively. However, its unstable native oxide makes its passivation a  
27  
28 21 crucial step towards its potential integration into future FETs. The  
29  
30 22 International Roadmap for Devices and Systems (IRDS™) predicts  
31  
32 23 continued aggressive scaling not only of the device size but also of the pitch  
33  
34 24 in nanowire arrays. The development of a vapor-phase chemical passivation  
35  
36 25 technique will be required to prevent the collapse of these structures that can  
37  
38 26 occur due to the surface tension and capillary forces that are experienced  
39  
40  
41  
42  
43  
44  
45  
46  
47  
48

1  
2  
3 27 when tight pitched nanowire arrays are processed via liquid-phase chemistry.  
4  
5 28 Reported here, is a vapor-phase process using hexanethiol for the passivation  
6  
7  
8 29 of planar Ge(100) substrates. Results benchmarking it against its well-  
9  
10 30 established liquid-phase equivalent are also presented. X-ray photoelectron  
11  
12 31 spectroscopy (XPS) was used to monitor the effectiveness of the developed  
13  
14 32 vapor-phase protocol where the presence of oxide was monitored at 0 h, 24  
15  
16  
17 33 h and 168 h. Water contact angle (WCA) measurements compliment these  
18  
19 34 results by demonstrating an increase in hydrophobicity of the passivated  
20  
21 35 substrates. Atomic force microscopy (AFM) monitored the surface topology  
22  
23 36 before and after processing to ensure the process does not cause roughening  
24  
25  
26 37 of the surface, which is critical to demonstrate suitability for nanostructures.  
27  
28 38 It is shown that the 200 minute vapor-phase passivation procedure generates  
29  
30 39 stable, passivated surfaces with less roughness than the liquid-phase  
31  
32  
33 40 counterpart.

### 41 **Introduction:**

42 Silicon (Si) is an essential part of modern technology since it forms the  
43 basis of the integrated circuits that are found in electronic devices. It also  
44  
45  
46  
47  
48

1  
2  
3 44 plays a critical role in infrared sensors,[1] solar panels [2] and chemical  
4  
5 45 sensors[3] and has been the semiconductor of choice for more than 60 years,  
6  
7 46 owing to its relative abundance, mechanical strength and stable native oxide.  
8  
9  
10 47 However, as the need for faster, more efficient processors grows, other  
11  
12 48 materials [4-7] and novel architectures [8] are being studied with the  
13  
14 49 intention that they be incorporated in devices alongside Si.

16  
17 50 As mentioned, germanium (Ge) is an attractive candidate as a channel  
18  
19 51 material, however, the germanium's native oxide is a complex system with a  
20  
21 52 range of oxidation states (+1, +2, +3, +4).[9] The bulk of this oxide,  $\text{GeO}_2$ ,  
22  
23 53 is problematic from a device perspective since it is unstable and the interface  
24  
25 54 between it and the underlying Ge is characterized by defects which lead to  
26  
27 55 charge trapping and poor overall device performance.[10] In FET devices,  
28  
29 56 the interface between the dielectric and the underlying channel material is  
30  
31 57 critical to the operation of the device. Ultimately, it is the nature of the native  
32  
33 58 oxide that has hindered the practical use of Ge to date.  $\text{GeO}_2$  can be removed  
34  
35 59 by treating the Ge with a halide acid (most commonly HF or HCl) solution,  
36  
37  
38 60 however, the resulting H-terminated or Cl-terminated Ge surfaces have been  
39  
40  
41  
42  
43  
44  
45  
46  
47  
48

1  
2  
3 61 shown to rapidly reoxidize upon exposure to the ambient.[11-13] It is for this  
4  
5 62 reason that the oxide must be removed and replaced with a passivating layer  
6  
7  
8 63 which inhibits re-oxidation such that a more reliable dielectric can be  
9  
10 64 deposited on the passivated Ge surface.

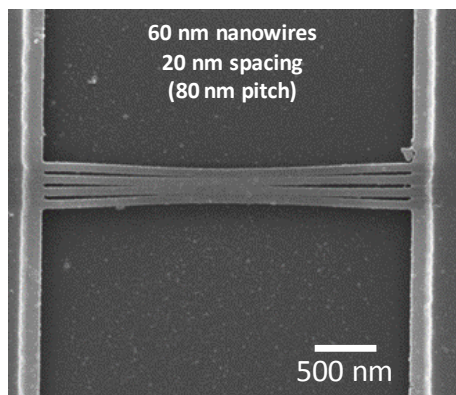
11  
12 65 There have been a number of reports on the passivation of Ge using liquid-  
13  
14 66 phase chemistry. Cullen *et al.* first reported the liquid-phase chemical  
15  
16  
17 67 functionalization of a Cl-terminated Ge surface using ethyl Grignard in  
18  
19 68 1962.[14] Choi and Buriak then demonstrated the hydrogermylation of H-  
20  
21 69 terminated Ge which mirrored the hydrosilylation reactions which had been  
22  
23  
24 70 carried out on Si.[15] Hanrath *et al.* have subsequently shown that the  
25  
26 71 hydrogermylation reaction is applicable to H-terminated Ge nanowires  
27  
28 72 also.[16] Both the Grignard chemistry and the hydrogermylation reaction  
29  
30  
31 73 result in a Ge-C bond. Alkanethiol liquid-phase chemistry has also been  
32  
33 74 developed for Ge which results in the formation of a Ge-S bond.[17] The  
34  
35 75 vapor-phase passivation of Group IV semiconductors has also been explored  
36  
37  
38 76 and dates back to the early 1960's whereby Si and Ge were passivated by  
39  
40 77 halides [14, 18-23], a range of organics [13, 24-29], nitrides and oxynitrides  
41  
42  
43  
44  
45  
46  
47  
48

1  
2  
3 78 [30-33]. For example, Degen *et al.* have reported the vapor-phase passivation  
4  
5 79 of Si(100) and Si(111) using short-chain alkynes for NEMS and MEMS  
6  
7  
8 80 devices.[34] Kosuri *et al.* have described the adsorption kinetics of 1-decyene  
9  
10 81 on H-terminated Si(100)[35] and Si(111)[36] and also the adsorption kinetics  
11  
12 82 of 1-alkanethiols on Ge(111)[37] surfaces. Takenaka *et al.* have reacted Ge  
13  
14 83 surfaces with vaporized tertiarybutylarsine (TBA) which is an arsenic source  
15  
16 84 for Ge doping.[38, 39] In this report, a facile approach for the vapor-phase  
17  
18  
19 85 passivation of oxide-free, chlorine-terminated Ge(100) using a short-chain  
20  
21 86 alkanethiol (1-hexanethiol) at ambient pressure and low temperature (140°C)  
22  
23  
24 87 is demonstrated.

25  
26  
27 88 The International Roadmap for Devices and Systems (IRDS™) predicts  
28  
29 89 that the fin/nanowire diameter, channel length and fin/nanowire pitch of these  
30  
31 90 devices will all decrease in size from one technology node to another.[40]  
32  
33  
34 91 The greatest predicted decrease in size is in the fin/nanowire pitch. Vapor-  
35  
36 92 phase passivation routes offer the ability to passivate structures with small  
37  
38 93 dimensions and pitches without causing the damage that liquid-phase  
39  
40  
41 94 alternatives can cause. An example of the impact of liquid-phase chemical  
42  
43  
44  
45  
46  
47  
48



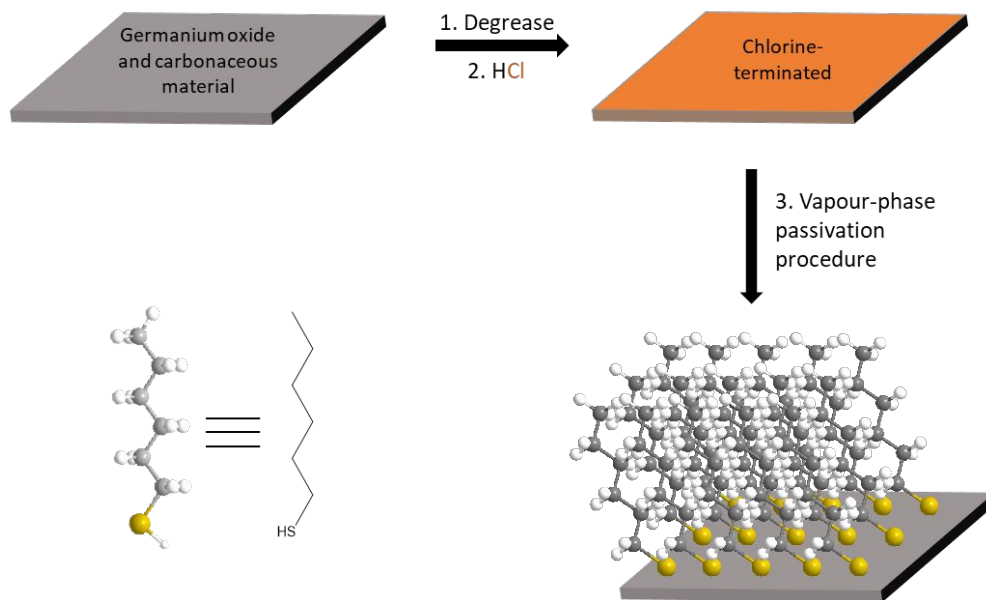
1  
2  
3 95 processing on the structure of suspended nanostructures can be seen in  
4  
5 96 **Figure 1**, where released Si nanowires have stuck together due to capillary  
6  
7 97 forces, after dipping in an aqueous solution of hydrofluoric acid (HF). An  
8  
9 98 example of a novel liquid-phase approach that has been shown to be effective  
10  
11 99 at passivating nanostructures is to conduct the passivation reactions in a  
12  
13 100 critical-point drier as demonstrated by Tao *et al.* for the alkylation and  
14  
15 101 amination of Si.[41] Alternatively, vapor-phase alternatives such as the one  
16  
17 102 documented here, can be implemented.  
18  
19  
20  
21  
22 103



104

1  
2  
3 105 **Figure 1.** SEM image of 60 nm long Si nanowires with a 20 nm spacing after  
4  
5 106 dipping in HF highlighting the effect of the capillary forces experienced  
6  
7 107 during liquid-phase processing  
8  
9

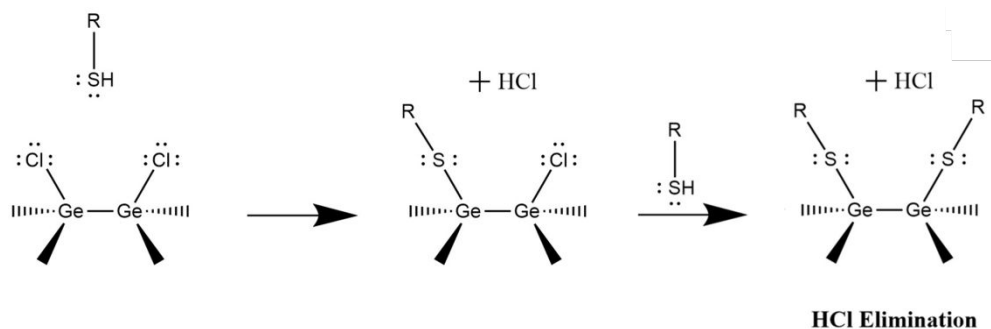
10  
11 108 To date, the bulk of the work carried out on self-assembled monolayers  
12  
13 109 (SAMs) on Ge has focused on using dodecanethiol, which has 12 carbon  
14  
15 110 atoms, to form SAMs on the Ge surface.[37, 42, 43] The preference for this  
16  
17 111 work was to choose a thiol molecule with the highest vapor pressure possible  
18  
19 112 (to enable effective vaporization) while still forming good quality  
20  
21 113 monolayers. A range of aliphatic thiol molecules with carbon backbones  
22  
23 114 ranging in length from 2 to 12 carbons were investigated for their ability to  
24  
25 115 passivate Ge and inhibit oxidation of the underlying Ge in 24 hours (see  
26  
27 116 **Figure S1**). Hexanethiol (HT) was ultimately chosen as the aliphatic thiol  
28  
29 117 molecule to passivate Ge in this study due to its relatively high vapor pressure  
30  
31  
32 118 and effective passivation of Ge.  
33  
34  
35  
36  
37  
38  
39  
40  
41  
42  
43  
44  
45  
46  
47  
48



**Scheme 1.** Schematic of oxide removal and passivation procedure for Ge using hexanethiol

A SAM is formed when a single layer of molecules bonds to a surface in a self-limiting fashion to yield a surface that is chemically stable. Herein, HT molecules are reacted in the vapor-phase with a Cl-terminated Ge(100) surface. A mechanistic explanation for what occurs during the 1-alkanethiol passivation of Cl-terminated Ge(100) has been discussed by Bent *et al.*[13] They explore three possible routes for the passivation; namely a

1  
2  
3 128 hydrohalogenic elimination pathway, an elimination and subsequent  
4  
5 129 insertion pathway and a pathway which involves the cleavage of the dimer  
6  
7 130 bond between Ge atoms at the surface. Their density functional theory  
8  
9 131 calculations show that adsorption of 1-alkanethiols on halide-terminated Ge  
10  
11 132 surface via hydrohalogenic acid elimination (**Figure 2**) is kinetically  
12  
13 133 favorable at room temperature. Thus, the reaction of HT with Cl-terminated  
14  
15 134 Ge(100) is likely to occur via this pathway and the Ge dimer bond is likely  
16  
17 135 to remain unbroken.[13]  
18  
19  
20  
21  
22



136

137 **Figure 2:** Proposed HCl elimination pathway for thiol reaction with Cl-  
138 terminated Ge

1  
2  
3 139 The reaction between the Cl-terminated Ge(111) surface and alkanethiol  
4  
5 140 molecules was also observed by Bent et al. and although not calculated  
6  
7  
8 141 directly, they expect hydrohalogenic acid elimination reactions similar to  
9  
10 142 those at halogenated Ge(100) to be kinetically favorable at halogenated  
11  
12 143 Ge(111) surfaces. Bent et al. observed the same general thiolation trends for  
13  
14 144 Ge(100) and Ge(111) surfaces however, there were some differences. After  
15  
16  
17 145 the thiolation reaction, higher levels of both sulfur and carbon were detected  
18  
19 146 at the Ge(100) surface, which indicated higher conversion of surface halides  
20  
21  
22 147 to surface thiolates on Ge(100) than on Ge(111).[13] With that said, the  
23  
24 148 thiolation of Cl-terminated Ge surfaces occurs for both Ge(100) and (111)  
25  
26 149 surfaces. The literature on the thiolation of other facets of Cl-terminated Ge  
27  
28  
29 150 is sparse however it has been shown for H-terminated Ge(110) surfaces that  
30  
31 151 thiol passivation is achieved.[44] Consideration of the passivation of various  
32  
33 152 facets of Ge is important in the context of both Ge nanostructures and planar  
34  
35 153 Ge surfaces. In relation to nanostructures, the top of the structure may be  
36  
37  
38 154 Ge(100), but crystal orientation of the sidewalls will vary depending on the  
39  
40 155 selectivity of etch used in their fabrication. In relation to planar Ge, it is  
41  
42  
43  
44  
45  
46  
47  
48

1  
2  
3 156 important to recognize that the Ge(100) surfaces used in this study are not  
4  
5 157 atomically flat (**Figure 4 (i)**) and that microfacets that locally resemble  
6  
7 158 Ge(111) and higher index surfaces are invariably present. With that said, the  
8  
9 159 studies, as described above, carried out on varied facets indicate that the  
10  
11 160 reaction always proceeds, even if the coverage varies somewhat.  
12  
13  
14

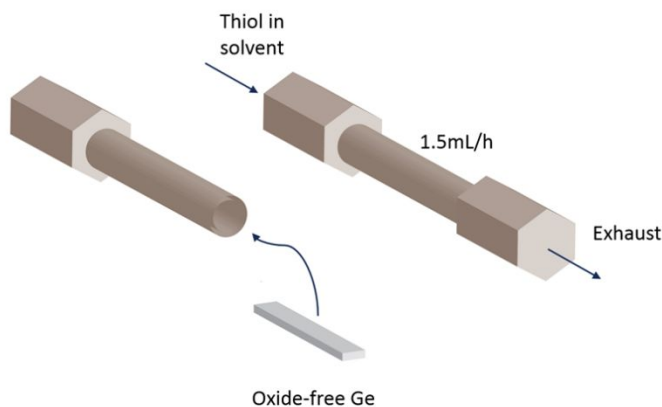
15  
16 161 A common use for SAMs on Ge is to inhibit the growth of the unreliable  
17  
18 162 oxide.[42, 43] In this study, the authors demonstrate a method to passivate  
19  
20 163 oxide free, Cl-terminated Ge(100) using HT in the vapor-phase. This method  
21  
22 164 is shown to be effective at preventing the regrowth of native Ge oxide for 24  
23  
24  
25 165 hours.  
26  
27

## 28 166 **Methods:**

29  
30

31 167 All chemicals were purchased from Sigma-Aldrich unless otherwise stated.  
32  
33 168 P-type germanium wafers were purchased from Umicore. Ge wafers were cut  
34  
35 169 into 1 cm<sup>2</sup> coupons and degreased by sonication in acetone for 3 minutes then  
36  
37 170 rinsed in IPA and dried under a stream of N<sub>2</sub>. GeO<sub>2</sub> was removed by dipping  
38  
39 171 the coupons in 20% HCl for 10 minutes followed by drying under N<sub>2</sub>. To  
40  
41  
42  
43  
44  
45  
46  
47  
48

1  
2  
3 172 achieve vapor-phase passivation, the coupons were loaded into a HiP MS  
4  
5 173 series micro reactor (**Figure 3**) in a glovebox with an atmosphere of  $< 0.5\text{ppm}$   
6  
7 174  $\text{O}_2$  and  $\text{H}_2\text{O}$ . The reactor was assembled in the glovebox to ensure no water  
8  
9 175 vapor was present which could have oxidized the chlorine-terminated, oxide-  
10  
11 176 free Ge prior to the vapor-phase thiol reaction. The assembled reactor was  
12  
13 177 then connected to HiP three way/two stem connection valves on both the inlet  
14  
15 178 and exhaust. The reactor was then loaded into a furnace.



38  
39  
40  
41 182  
42  
43  
44  
45  
46  
47  
48

180 **Figure 3.** Schematic of HiP MS series micro reactor configuration

181 A 0.1M solution of thiol in toluene was degassed using the freeze-pump-  
182 thaw (FPT) method. This method involves freezing the thiol solution under

1  
2  
3 183 N<sub>2</sub> using liquid nitrogen and then allowing the solution thaw under vacuum  
4  
5 184 (10<sup>-3</sup> Torr) to remove undesirable gases present in the solvent. This method  
6  
7  
8 185 was repeated 3 times - until there was no more evolution of gas from the thiol  
9  
10 186 solution. The degassed thiol solution was then syringed from the round-  
11  
12 187 bottom flask using a 10 mL Luer-lock syringe which had been dried in a  
13  
14 188 vacuum oven at 60°C overnight and then purged with N<sub>2</sub> prior to filling with  
15  
16  
17 189 the thiol solution. The Luer-lock syringe was used to pump the thiol solution  
18  
19 190 at 1.5 mL/hr into the reactor at 140°C, carried by a constant flow of H<sub>2</sub> in Ar.  
20  
21 191 After 200 minutes, the furnace was turned off and the injection of the thiol  
22  
23 192 solution into the reactor was stopped. At this point, 5 mL of the thiol solution  
24  
25  
26 193 had been pumped through the reactor. The reactor was then allowed to cool  
27  
28 194 for 30 minutes before the samples were removed. The samples were then  
29  
30  
31 195 sonicated in acetone for 5 minutes, rinsed with propanol and dried under a  
32  
33 196 stream of N<sub>2</sub>. For comparison, a liquid-phase chemical procedure for  
34  
35 197 passivation of Ge was conducted also. In this case, a 0.1M solution of HT in  
36  
37  
38 198 toluene was degassed using the FPT method described previously. Oxide-  
39  
40 199 free, Cl-terminated Ge samples were refluxed in the solution under an N<sub>2</sub>  
41  
42  
43  
44  
45  
46  
47  
48



1  
2  
3 200 atmosphere using Schlenk line apparatus for 24 hours as is common in the  
4  
5 201 literature to achieve thiol SAMs of high quality on Ge.[13, 29, 43] Samples  
6  
7 202 were exposed to 40% relative humidity (RH) at 20°C in a Votsch temperature  
8  
9 203 test chamber to emulate ambient conditions for 24 hours to track what affect  
10  
11 204 the ambient had on the samples.  
12  
13  
14

15 205 Atomic force microscopy was used to determine if the processing affected  
16  
17 206 surface roughness. Water contact angle analysis was used to determine the  
18  
19 207 hydrophobicity of the sample surface which gives an indication of the quality  
20  
21 208 of the SAM and X-ray photoelectron spectroscopy was used to get elemental  
22  
23 209 analysis of the Ge surface post reaction and after exposure to the ambient for  
24  
25 210 24 hours to determine if the passivated surface was resistant to oxidation.  
26  
27 211 Passivated samples were transported under a positive pressure of N<sub>2</sub> in a SPI-  
28  
29 212 DRY™ Sample Preserver to the characterization tools.  
30  
31  
32  
33  
34

### 35 213 1. Atomic Force Microscopy (AFM)

36  
37

38 214 All AFM measurements in this study were taken using tapping mode Veeco  
39  
40 215 Multimode V at room temperature over a 3 x 3 μm<sup>2</sup> scanning area. Tapping  
41  
42  
43  
44  
45

1  
2  
3 216 mode is preferred to contact mode when working with SAMs since the SAM  
4  
5 217 can be affected by the probe being in constant contact with the surface.  
6  
7  
8 218 Tapping mode bypasses this problem since the probe is not dragged along  
9  
10 219 the surface.  
11  
12

## 13 220 2. Water Contact Angle (WCA)

14  
15

16 221 An image of a 50  $\mu\text{L}$  drop of deionized water on the Ge surface was  
17  
18 222 obtained and the angle formed between the water, Ge surface and air was  
19  
20 223 measured. The greater the angle, the more hydrophobic the sample. Here, the  
21  
22 224 wettability of a Ge surface gives an indication as to whether the thiol  
23  
24 225 molecule has reacted with that surface. Considering the tail of the HT  
25  
26 226 molecule is non-polar in nature, an increase in hydrophobicity indicates that  
27  
28 227 a thiol SAM is present on the Ge surface.  
29  
30  
31  
32

## 33 228 3. X-Ray Photoelectron Spectroscopy (XPS)

34  
35  
36

37 229 XPS spectra were acquired on an Oxford Applied Research Escabase XPS  
38  
39 230 System equipped with a CLASS VM 100 mm mean radius hemispherical  
40  
41 231 electron energy analyzer with multichannel detectors in an analysis chamber  
42  
43  
44  
45  
46  
47  
48

1  
2  
3 232 with a base pressure of  $5.0 \times 10^{-9}$  mbar. A pass energy of 50 eV, a step size  
4  
5 233 of 0.7 eV and a dwell of 0.3 s was used for survey spectra which were swept  
6  
7  
8 234 twice. All core level scans other than the S 2p and 2s were acquired with a  
9  
10 235 step size of 0.1 eV, a dwell time of 0.1 s and a pass energy of 20 eV averaged  
11  
12 236 over 10 scans. The S 2p and 2s scans were acquired with a step size of 0.1  
13  
14 237 eV, a dwell time of 0.1 eV and a pass energy of 50 eV averaged over 20  
15  
16  
17 238 scans. This was done to maximize the intensity of the S 2p peaks so accurate  
18  
19 239 peak fitting could be carried out. A non-monochromated Al-K $\alpha$  X-ray source  
20  
21 240 (1486.58 eV) at 100 W power (10 mA, 10kV) was used for all scans. All  
22  
23  
24 241 spectra were acquired at a take-off angle of 90° with respect to the analyzer  
25  
26 242 axis and were charge corrected with respect to the C 1s photoelectric line at  
27  
28 243 284.8 eV. A Shirley type background was used for construction and peak  
29  
30  
31 244 fitting of synthetic peaks. Synthetic peaks were a mix of Gaussian-Lorentzian,  
32  
33 245 the Ge 2p spectra were fit using Gaussian-Lorentzian peak shape GL(90) for  
34  
35 246 the elemental Ge peak and Lorentzian peak shape LA(1.53,243) for all other  
36  
37  
38 247 peaks. The relative sensitivity factors used are from a CasaXPS library  
39  
40 248 containing Scofield cross-sections.  
41  
42  
43  
44  
45  
46  
47  
48

1  
2  
3 249 **Results & Discussion:**  
4

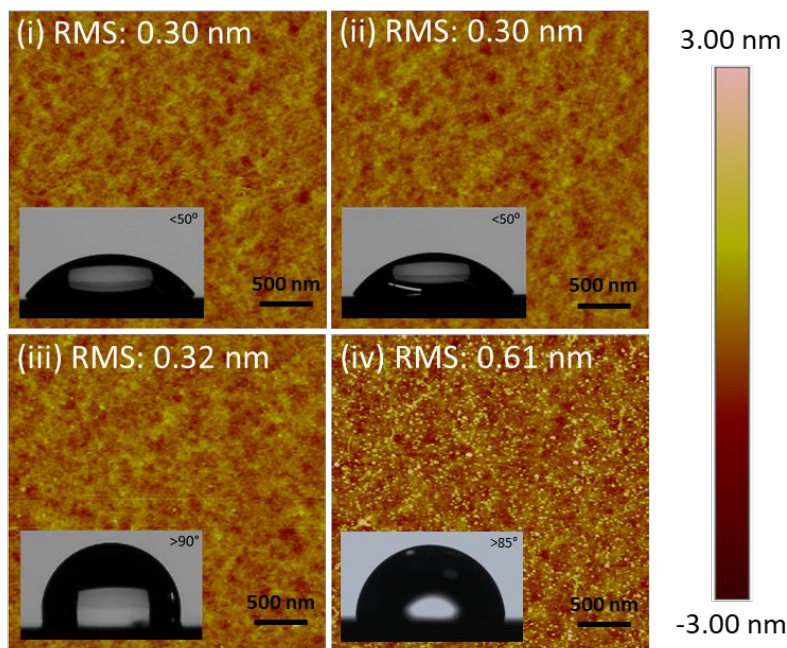
5  
6 250 *Atomic Force Microscopy & Water Contact Analysis:*  
7

8  
9  
10 251 An industry requirement for the passivation of Ge is that its surface remains  
11  
12 252 oxide-free for a queue-time of 24 hours. This allows for maintenance or  
13  
14 253 repair of instrumentation, which may result in the exposure of processed Ge  
15  
16 254 to the ambient during device fabrication. Processed Ge wafers require a  
17  
18 255 sufficiently robust passivation layer to avoid reoxidation of the substrates.  
19  
20  
21 256 Processes developed on planar Ge must be non-destructive such that they be  
22  
23 257 transferrable to highly ordered, densely packed, high aspect-ratio Ge  
24  
25  
26 258 nanostructures. As a result, AFM was used to track the effect the processing  
27  
28 259 had on the roughness of planar Ge surfaces. Since the surface to bulk ratio  
29  
30 260 for nanostructures is high, it is imperative that any processing has a negligible  
31  
32 261 impact on surface roughness. Results for the liquid-phase passivation of Ge  
33  
34  
35 262 using HT are included for comparison.  
36  
37

38 263 Prior to the vapor-phase passivation of the Ge surface, the native oxide was  
39  
40 264 removed using a 20% solution of HCl. This step relies on wet chemical  
41  
42  
43  
44  
45  
46  
47  
48

1  
2  
3 265 processing which would not be compatible with nanostructures, however in  
4  
5 266 the context of an industrial setting a vapor phase alternative would be applied.  
6  
7  
8 267 The RMS value obtained for a clean Ge surface is 0.30 nm as seen in **Figure**  
9  
10 268 **4 (i)**. The inset in **Figure 4 (i)** highlights how the surface prior to any  
11  
12 269 processing is hydrophilic, a shallow angle of less than  $50^\circ$  is obtained when  
13  
14 270 a 50  $\mu$ L drop of millipore deionized water is deposited onto the surface. This  
15  
16 271 value is consistent for literature values of ultrasonic cleaned Ge surfaces.[48]  
17  
18  
19 272 The surface is hydrophilic since the water interacts favorably with the  $\text{GeO}_2$   
20  
21 273 film present on the surface. After the HCl etch, a Cl-terminated Ge surface  
22  
23 274 with an RMS value of 0.30 nm was obtained. Removing the oxide with HCl  
24  
25 275 does not cause an increase in the surface roughness. The inset in **Figure 4 (ii)**  
26  
27 276 illustrates how the chlorine-terminated Ge surface is also hydrophilic. A  
28  
29 277 water contact angle of less than  $50^\circ$  is obtained since the water molecules  
30  
31 278 interact favorably with the Cl-terminated Ge surface. This is consistent with  
32  
33 279 the literature on Cl-terminated Ge whereby angles of  $39\text{-}50^\circ$  are  
34  
35 280 observed.[48, 49] The AFM image in **Figure 4 (iii)**, illustrates how the vapor-  
36  
37 281 phase HT passivation reaction does not cause an increase in Ge surface  
38  
39  
40  
41  
42  
43  
44  
45  
46  
47  
48

1  
2  
3 282 roughness and the degree of hydrophobicity of the Ge surface sharply  
4  
5 283 increases to over 90°. Increasing contact angle measurements for alkanethiol  
6  
7  
8 284 SAMs have been shown to correlate with the length of the alkanethiol  
9  
10 285 molecule.[46] On Ge(100), alkanethiol SAMs consisting of 1-dodecanethiol  
11  
12 286 molecules have been shown to display WCA of > 100°,[42] while SAMs  
13  
14  
15 287 consisting of 1-octadecanethiol molecules (C18) have been shown to display  
16  
17 288 WCA of > 115°.[50] In this study, HT, having a shorter C backbone, was  
18  
19 289 found to form a SAM on Ge that yield a surface with a WCA of 90°. The  
20  
21  
22 290 sharp increase in the hydrophobicity of the Ge surface is a clear indication  
23  
24 291 that the vapor-phase reaction occurred between the Cl-terminated Ge surface  
25  
26 292 and the HT molecules. For comparison, the AFM and WCA data for a Ge  
27  
28  
29 293 surface which has been passivated using the liquid-phase chemistry approach  
30  
31 294 have been included also. It is clear from the AFM image in **Figure 4 (iv)** that  
32  
33 295 the surface roughness of the Ge is affected by the liquid-phase passivation  
34  
35 296 procedure where an RMS value of 0.61 nm is observed along with a WCA  
36  
37  
38 297 of 85°. The increased WCA indicates that a HT SAM is present on the  
39  
40 298 surface.  
41  
42  
43  
44  
45  
46  
47  
48



299

300 **Figure 4.** AFM images with water contact angle insets of (i) as-rec Ge (ii)  
301 HCl treated Ge (iii) HT vapor-phase passivated Ge with 0 hours exposure to  
302 the ambient (iv) HT liquid-phase passivated Ge with 0 hours exposure to the  
303 ambient

304 *X-ray Photoelectron Spectroscopy characterization:*

305 In the literature, when discussing the oxidation of Ge, it is common to  
306 discuss the Ge 3d peak primarily; however, the 3d transition comes from

1  
2  
3 307 electrons with high kinetic energy and therefore from a greater sampling  
4  
5 308 depth when compared to the electrons from the 2p transition which have  
6  
7  
8 309 lower kinetic energy and so are more surface sensitive. Thus, in an attempt  
9  
10 310 to highlight what is occurring at the surface of the Ge, the Ge 2p peak will be  
11  
12 311 presented in this study. When fitting the oxide peaks, the suboxide peak  
13  
14 312 position was fixed at 1.1 eV greater than the elemental Ge peak. GeO<sub>2</sub> peak  
15  
16 313 position was not fixed since a trend was observed whereby the peak position  
17  
18 314 shifted to higher binding energy upon oxidation. Oxide thickness was  
19  
20  
21 315 calculated using the method outlined by Murakami *et al.*[51]  
22  
23  
24

25  
26 316 
$$d_{GeO_2} = \lambda_{GeO_2} \sin\theta \ln\left(\frac{I_{Ge}^\infty I_{GeO_2}}{I_{GeO_2}^\infty I_{Ge}} + 1\right)$$
  
27  
28  
29

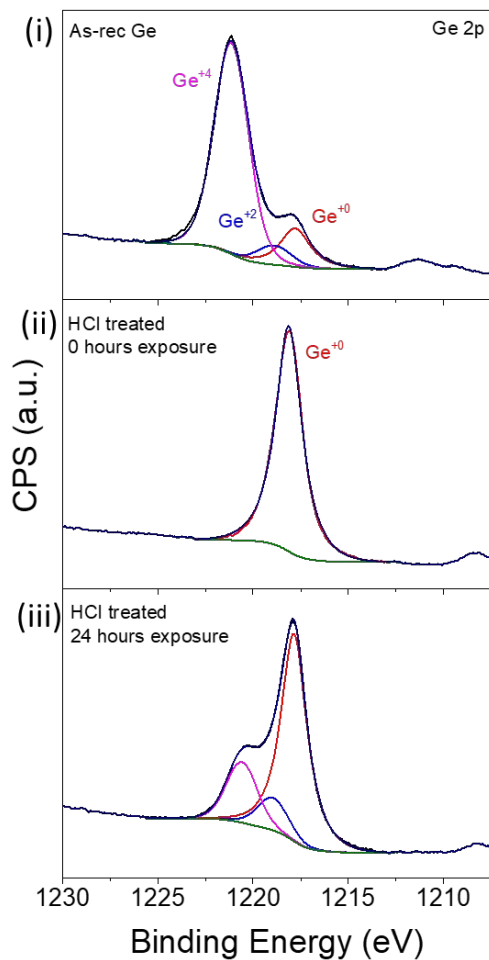
30 317 Where  $\lambda_{GeO_2}$ , the inelastic mean free path for the Ge 2p transition is 0.9 nm;  
31  
32 318 the photoemission angle  $\theta$  is 90°;  $I_{Ge}^\infty/I_{GeO_2}^\infty$  is the ratio of the Ge 2p signal  
33  
34 319 from infinitely thick Ge to infinitely thick GeO<sub>2</sub> and is determined as 1.73;  
35  
36 320  $I_{GeO_2}$  is the intensity of the of native oxide (GeO<sub>2</sub>) peak from curve fitting the  
37  
38 321 Ge 2p transition;  $I_{Ge}$  is the intensity of the metallic Ge peak from curve fitting  
39  
40  
41  
42  
43  
44  
45  
46  
47  
48



1  
2  
3 322 the Ge 2p transition. This calculation was repeated to determine the thickness  
4  
5 323 of the suboxide ( $\text{GeO}_x$ ) component for each sample also. In this case,  $I_{\text{GeO}_x}$ ,  
6  
7  
8 324 the fraction of suboxide ( $\text{GeO}_x$ ) from curve fitting the Ge 2p was used in  
9  
10 325 place of  $I_{\text{GeO}_2}$ .

11  
12  
13  
14 326 **Figure 5 (i)** depicts the Ge 2p spectrum for an as-received Ge sample that  
15  
16 327 has undergone no processing. As expected, there is a large peak at 1221.14  
17  
18 328 eV that corresponds to  $\text{Ge}^{+4}$  from  $\text{GeO}_2$ . There is also a peak evident at  
19  
20 329 1218.89 eV which is attributed to the suboxide, GeO. The thickness of the  
21  
22  
23 330  $\text{GeO}_2$  on as-rec Ge is 2.12 nm which is in agreement with literature values  
24  
25 331 for as-rec Ge(100).[52] The thickness of the suboxide component was 0.56  
26  
27 332 nm. The suboxide component of Ge likely has contributions from Ge in +1,  
28  
29 333 +2 and +3 states however these cannot be accurately resolved with the  
30  
31  
32 334 instrumentation available. Treatment of the as-received Ge with HCl  
33  
34 335 removed both the native oxide and the suboxide component leaving a Cl-  
35  
36 336 terminated surface which oxidized upon exposure to the ambient. This is  
37  
38  
39 337 evident in **Figure 5 (ii, iii)** where the Ge 2p peaks corresponding to the native  
40  
41 338 oxide and suboxide are no longer present after the HCl dip but return after 24  
42  
43  
44  
45  
46  
47  
48

1  
2  
3 339 hours of exposure to the ambient. A GeO<sub>2</sub> film, 0.34 nm thick grows in 24  
4  
5 340 hours of exposure to the ambient indicating that Cl-termination does not  
6  
7 341 sufficiently prevent reoxidation of the Ge surface.  
8  
9  
10  
11  
12  
13  
14  
15  
16  
17  
18  
19  
20  
21  
22  
23  
24  
25  
26  
27  
28  
29  
30  
31  
32  
33  
34  
35  
36  
37  
38  
39  
40  
41  
42  
43  
44  
45  
46  
47  
48

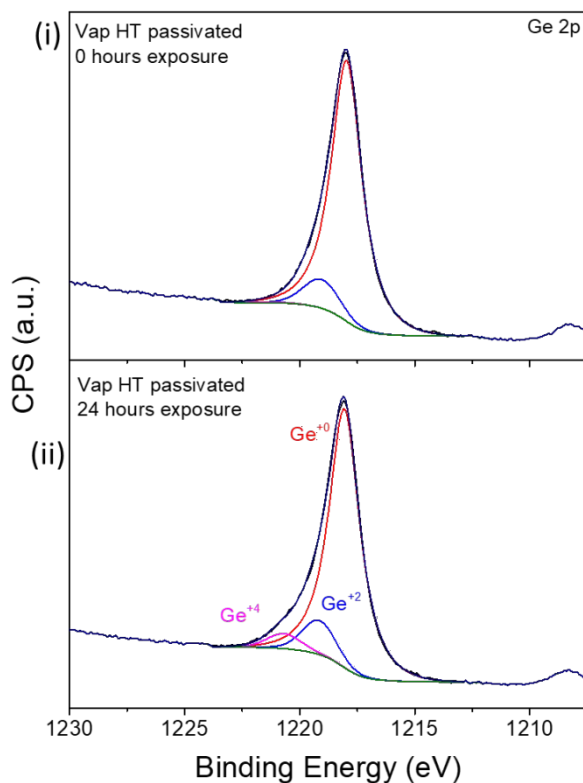


342

343 **Figure 5.** Ge 2p plots for (i) as-rec Ge (ii) and (iii) Cl-terminated Ge after 0  
344 and 24 hours exposure to the ambient respectively

1  
2  
3 345 **Figure 6 (i)** depicts the Ge 2p spectra for a Ge sample that has had the  
4  
5 346 native oxide removed by a HCl etch followed by passivation using HT in the  
6  
7 347 vapor-phase. No GeO<sub>2</sub> is detected after the passivation reaction however,  
8  
9 348 there is a component at 1219.2 eV which is likely attributable to Ge<sup>+2</sup> from a  
10  
11 349 mixture of Ge-O and Ge-S after the passivation reaction. An XPS tool with  
12  
13 350 higher resolution would be needed to attempt to resolve these components.  
14  
15 351 The calculated thickness of these components is 0.16 nm. After 24 hours of  
16  
17 352 exposure to the ambient, the GeO<sub>2</sub> film thickness was 0.08 nm. The growth  
18  
19 353 of oxide is minimal and as such can be used as a proxy for quality of SAM  
20  
21 354 on the Ge surface. The more stable and uniform the SAM, the slower the  
22  
23 355 growth of oxide. In this case, the vapor-phase passivated Ge exhibits  
24  
25 356 inhibition of oxide growth and thus one can infer that a stable SAM is present.  
26  
27 357 The peak at 1219.2 eV is still present after the passivation reaction is  
28  
29 358 unchanged with a calculated thickness of 0.16 nm. After 168 hours of  
30  
31 359 exposure to the ambient, GeO<sub>2</sub> thickness was calculated to be 0.25 nm with  
32  
33 360 the thickness of the component at 1219.2 eV calculated to be 0.20 nm  
34  
35 361 indicating that continued oxidation does occur albeit slowly. The thickness  
36  
37  
38  
39  
40  
41  
42  
43  
44  
45  
46  
47  
48

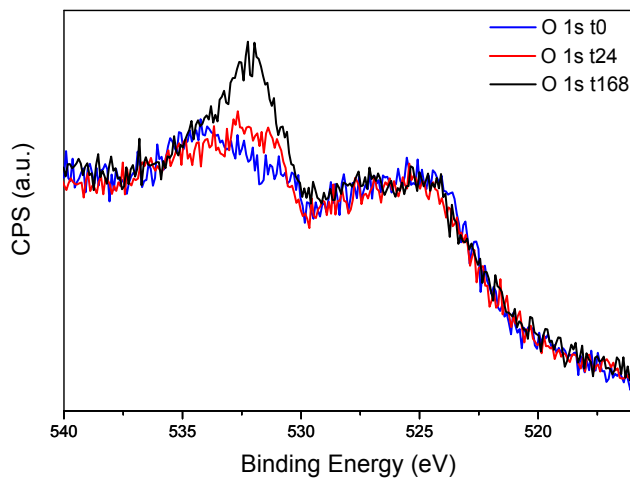
1  
2  
3 362 of the oxide film on the HT vapor-phase passivated sample after 168 hours  
4  
5 363 exposure to the ambient is less than that of the Cl-terminated sample after  
6  
7 364 only 24 hours of exposure (0.25 nm vs. 0.34 nm). The 168 hour Ge 2p  
8  
9 365 spectrum is presented in **Supporting Information** section (**Figure S3**).



366

1  
2  
3 367 **Figure 6.** (i) and (ii) Ge 2p plots for HT vapor-phase passivated Ge with 0  
4  
5 368 and 24 hours exposure to the ambient respectively  
6  
7

8 369 An inspection of the O 1s peaks for the vapor-phase passivated Ge directly  
9  
10 370 after the passivation reaction and after 24 and 168 hours of exposure to the  
11  
12 371 ambient is illustrated in **Figure 7**. There is little growth in the intensity of the  
13  
14 372 O 1s peak after 24 hours however after 168 hours some growth is observed  
15  
16 373 indicating that the HT SAM passivation is effective at inhibiting oxidation of  
17  
18 374 the Ge over 24 hours but that in the following 144 hours, a small amount of  
19  
20 375 GeO<sub>2</sub> growth occurs (0.17 nm growth in the 144 hours proceeding the first  
21  
22 376 24 hours).  
23  
24  
25  
26  
27  
28  
29  
30  
31  
32  
33  
34  
35  
36  
37  
38  
39  
40  
41  
42  
43  
44  
45  
46  
47  
48



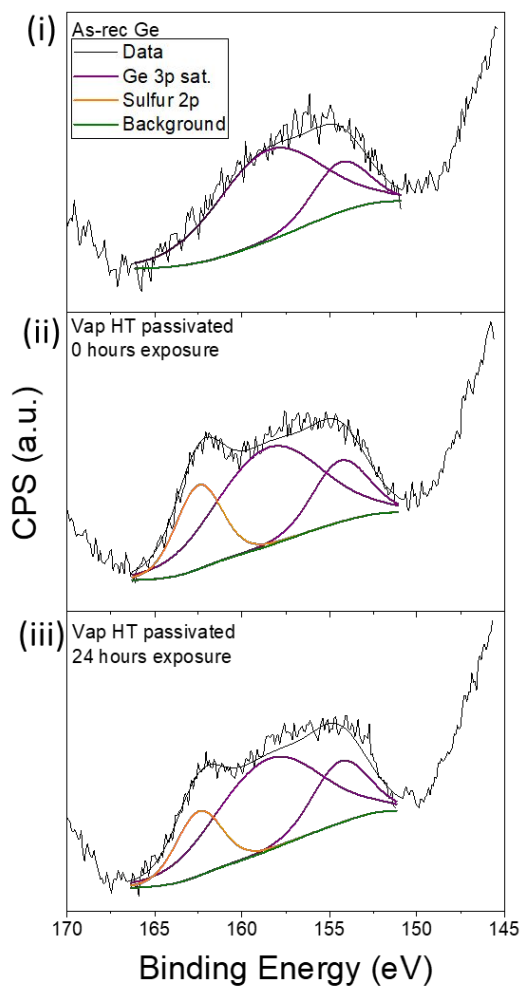
377

378 **Figure 7.** O 1s spectra of Ge passivated by HT in the vapor-phase after 0  
379 (blue), 24 (red) and 168 (black) hours exposure to the ambient

380 The S 2p peak occurs at 162.3 eV which overlaps with a Ge 3p satellite  
381 feature, however through peak fitting, the S 2p peak can be clearly  
382 differentiated from the Ge 3p sat. There is no S 2p peak present in the as-rec  
383 Ge sample (**Figure 8 (i)**), as expected. However, a clear S 2p peak is observed  
384 at 162.3 eV in **Figure 8 (ii)** for the HT passivated sample. That peak is still  
385 evident after 24 hours of exposure to the ambient (**Figure 8 (iii)**), albeit with  
386 slight lower intensity, which indicates that the thiol SAM is stable on the

1  
2  
3 387 surface for 24 hours. A possible explanation as to why the intensity of the S  
4  
5 388 2p peak diminishes slightly in 24 hours is that the growth of a small amount  
6  
7  
8 389 of oxide on the surface in 24 hours displaces the thiol molecules, resulting in  
9  
10 390 a slightly less intense S 2p peak. The XPS measurements showing the  
11  
12 391 presence of sulfur on the vapor-phase HT treated surface is clear indication  
13  
14 392 that the vaporized HT reacted with the Cl-terminated Ge surface. The  
15  
16  
17 393 presence of the S 2p peak after 24 hours and the minimal growth of oxide  
18  
19 394 observed in **Figure 6** indicates that the HT SAM on the Ge surface is stable  
20  
21 395 and more effective than chlorine at preventing oxidation from the ambient  
22  
23  
24 396 for 24 hours.  
25  
26  
27  
28  
29  
30  
31  
32  
33  
34  
35  
36  
37  
38  
39  
40  
41  
42  
43  
44  
45  
46  
47  
48

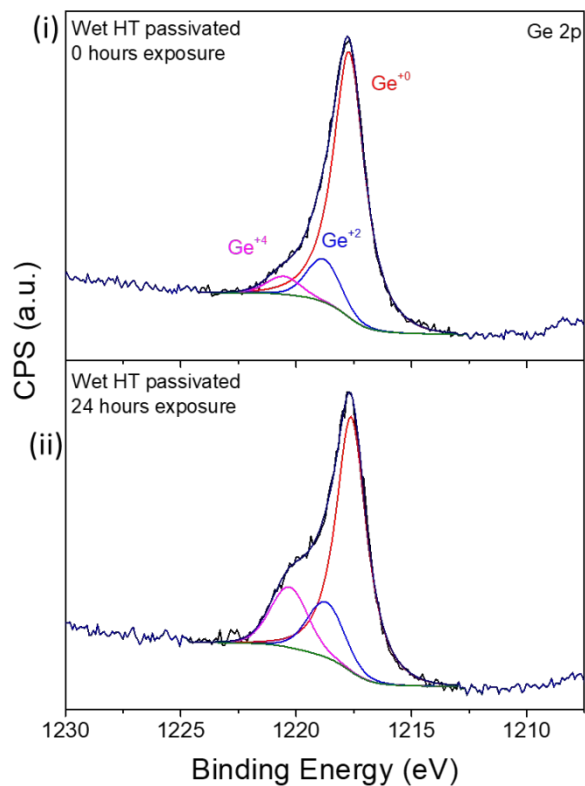




397

1  
2  
3 398 **Figure 8.** (i) as-rec Ge showing no S peak (ii) HT vapor-phase passivated Ge  
4  
5 399 with 0 hours exposure to the ambient (iii) HT vapor-phase passivated Ge with  
6  
7 400 24 hours exposure to the ambient  
8  
9

10  
11 401 For comparison with the vapor-phase passivation approach, **Figure 9**  
12  
13 402 elucidates the liquid-phase passivation of Ge, where some native oxide is  
14  
15 403 present directly after the passivation reaction and the oxide thickness is 0.21  
16  
17 404 nm. The presence of this oxide indicates that the during the 24-hour  
18  
19 405 processing, a small amount of Ge oxidation occurs. This is not the case with  
20  
21 406 the shorter (200 minute) vapor-phase reaction where there is no detectable  
22  
23 407 GeO<sub>2</sub> directly after the passivation reaction. Shorter processing times are  
24  
25 408 desirable since they decrease the likelihood that oxidation can occur. The  
26  
27 409 thickness of the oxide for the liquid-phase passivated sample increases to  
28  
29 410 0.34 nm after 24 hours of exposure to ambient conditions (a growth of 0.13  
30  
31 411 nm).  
32  
33  
34  
35  
36  
37  
38  
39  
40  
41  
42  
43  
44  
45  
46  
47  
48



412

413 **Figure 9.** (i) and (ii) Ge 2p spectra for the liquid-phase passivation of Ge  
414 illustrating the presence of native oxide after 0 and 24 hours exposure to the  
415 ambient respectively

1  
2  
3 416 This XPS data, coupled with the WCA data from **Figure 4** indicate that the  
4  
5 417 liquid-phase passivation reaction yields a SAM of which does not inhibit  
6  
7 418 oxidation of the Ge as effectively as the vapor-phase passivated sample. The  
8  
9 419 vapor-phase passivation method results eclipse those of the liquid-phase  
10  
11 420 chemical passivation in relation to oxidation inhibition over 24 hours of  
12  
13 421 exposure to the ambient. A summary of the oxide thicknesses is tabulated in  
14  
15 422 **Table 1.**  
16  
17  
18  
19

Sample	GeO <sub>2</sub> thickness (nm)	
	0 hrs exposure	24 hrs exposure
As-Rec	2.12	2.12
HCl treated Ge	0	0.38
Vap. HT Passivated Ge	0	0.08
Liq. HT Passivated Ge	0.21	0.34

1  
2  
3 **Table 1.** Oxide thicknesses for as-rec, HCl-treated, vapor-phase passivated  
4  
5 and liquid-phase passivated Ge(100) samples  
6

7  
8  
9 *Estimation of Overlayer Thickness:*

10  
11  
12 XPS thickness measurement of the SAM overlayer for the vapor-phase  
13  
14 passivated Ge was performed following the methodology originally defined  
15  
16 by Cumpson *et al.* [53]  
17

18  
19  
20  
21 
$$\ln\left(\frac{I_o S_o}{I_s S_s}\right) - \left(\frac{\lambda_o}{\lambda_s}\right) \frac{1}{\lambda_o \cos \theta} - \ln 2 = \ln \sin h\left(\frac{t}{2\lambda_o \cos \theta}\right)$$
  
22  
23  
24

25 where  $I_o$  and  $I_s$  represent the respective measured peak intensities of the  
26  
27 overlayer (HT molecules) and the substrate peaks,  $S_o$  and  $S_s$  refer to the  
28  
29 relative sensitivity factors for the overlayer and the substrate respectively.  $\lambda_o$   
30  
31 and  $\lambda_s$  are the attenuation lengths of electrons in the overlayer and the  
32  
33 substrate.  $\theta$  is the emission angle with respect to the surface normal. The peak  
34  
35 intensity of the overlayer peak,  $I_o$ , and the peak intensity of the substrate peak,  
36  
37  $I_s$ , were determined using CasaXPS software after a transmission correction.  
38  
39  
40  
41  
42 The relative sensitivity factors for the substrate peak  $S_s$  and the overlayer  
43  
44  
45  
46  
47  
48

1  
2  
3 438 peak  $S_{0s}$  were also obtained from the CasaXPS library and manually inputted  
4  
5  
6 439 into the data processing software to remove instrumental factors which may  
7  
8 440 affect quantification. The practical electron attenuation length (EAL) in the  
9  
10 441 overlayer,  $l_o$ , was estimated, using the NIST Electron Effective Attenuation  
11  
12 442 Length database, to be  $2.58 \pm 0.2$  nm for the Ge 3d component. Using this  
13  
14 443 method, the thickness of the SAM overlayer was estimated to be  
15  
16  
17 444 approximately 1 nm which is in accordance with the length of one HT  
18  
19 445 molecule – the expected thickness of the monolayer.  
20

21  
22  
23 **446 Conclusion:**  
24

25  
26 447 In this study, it has been shown that a facile and mild 200 minute vapor-  
27  
28 448 phase passivation reaction of Ge(100) using HT yields a Ge surface that  
29  
30 449 resists oxidation for 24 hours. The procedure does not cause an increase in  
31  
32  
33 450 surface roughness. The significance of this is apparent when considering Ge  
34  
35 451 nanostructures especially. This passivation procedure could be implemented  
36  
37 452 on structures that would otherwise be damaged by liquid-phase chemical  
38  
39  
40 453 processing – an important step on the road to realizing Ge's potential as a  
41  
42 454 channel material in modern devices.  
43  
44  
45

1  
2  
3 455 **Corresponding Author**  
4

5  
6 456 Dr. Brenda Long  
7

8  
9 457 **Author Contributions**  
10

11 458 The manuscript was written through contributions of all authors. All authors  
12  
13 459 have given approval to the final version of the manuscript.  
14  
15

16  
17 460 **Funding Sources**  
18

19  
20 461 The authors acknowledge financial support from Enterprise Ireland (EI IP  
21  
22 462 2018 0757A).  
23  
24

25 463 **Abbreviations**  
26

27 464 Ge, germanium; Si, silicon; SAM, self-assembled monolayer; XPS, x-ray  
28  
29 465 photoelectron spectroscopy; WCA, water contact angle; AFM, atomic force  
30  
31 466 microscopy; HT, hexanethiol; DoDT, dodecanethiol; HCl, hydrochloric acid;  
32  
33 467 HF, hydrofluoric acid.  
34  
35  
36

37 468 **Supporting Information**  
38

39 469 Ge 2p XPS spectra for a liquid-phase passivation of Ge by ethanethiol,  
40  
41 470 butanethiol, pentanethiol, hexanethiol, octanethiol and dodecanethiol. Ge 3d  
42  
43  
44

1  
2  
3 471 and S 2s XPS spectra for vapor-phase passivation of Ge by hexanethiol. Ge  
4  
5 472 2p XPS spectra for vapor-phase hexanethiol passivated Ge after 168 hours  
6  
7  
8 473 exposure to the ambient. XPS survey spectra.  
9

10  
11 474 **References**  
12  
13

- 14 475 1. Singh, V., P.T. Lin, N. Patel, H. Lin, L. Li, Y. Zou, F. Deng, C. Ni, J.  
15 476 Hu, J. Giammarco, A.P. Soliani, B. Zdyrko, I. Luzinov, S. Novak, J.  
16 477 Novak, P. Wachtel, S. Danto, J.D. Musgraves, K. Richardson, L.C.  
17 478 Kimerling, and A.M. Agarwal, *Mid-Infrared Materials and Devices*  
18 479 *on a Si Platform for Optical Sensing*. Science and Technology of  
20 480 Advanced Materials, 2014. **15**(1): p. 014603.  
21 481 2. Pillai, S., K.R. Catchpole, T. Trupke, and M.A. Green, *Surface*  
22 482 *Plasmon Enhanced Silicon Solar Cells*. Journal of Applied Physics,  
23 483 2007. **101**(9): p. 093105.  
24 484 3. Cui, Y., Q. Wei, H. Park, and C.M. Lieber, *Nanowire Nanosensors*  
25 485 *for Highly Sensitive and Selective Detection of Biological and*  
26 486 *Chemical Species*. Science, 2001. **293**(5533): p. 1289.  
27 487 4. Gupta, A., T. Sakhivel, and S. Seal, *Recent Development in 2D*  
28 488 *Materials Beyond Graphene*. Progress in Materials Science, 2015. **73**:  
29 489 p. 44-126.  
30 490 5. Manzeli, S., D. Ovchinnikov, D. Pasquier, O.V. Yazyev, and A. Kis,  
31 491 *2D Transition Metal Dichalcogenides*. Nature Reviews Materials,  
32 492 2017. **2**: p. 17033.  
33 493 6. Mirabelli, G., C. McGeough, M. Schmidt, E.K. McCarthy, S.  
34 494 Monaghan, I.M. Povey, M. McCarthy, F. Gity, R. Nagle, G. Hughes,  
35 495 A. Cafolla, P.K. Hurley, and R. Duffy, *Air Sensitivity of MoS<sub>2</sub>,*  
36 496 *MoSe<sub>2</sub>, MoTe<sub>2</sub>, HfS<sub>2</sub>, and HfSe<sub>2</sub>*. Journal of Applied Physics, 2016.  
37 497 **120**(12): p. 125102.  
38  
39  
40  
41  
42  
43  
44  
45  
46  
47  
48



- 1  
2  
3 498 7. Tomioka, K., M. Yoshimura, and T. Fukui, *A III–V Nanowire*  
4 499 *Channel on Silicon for High-Performance Vertical Transistors.*  
5 500 *Nature*, 2012. **488**(7410): p. 189-192.  
6 501 8. Su, C., T. Tsai, Y. Liou, Z. Lin, H. Lin, and T. Chao, *Gate-All-Around*  
7 502 *Junctionless Transistors With Heavily Doped Polysilicon Nanowire*  
8 503 *Channels.* *IEEE Electron Device Letters*, 2011. **32**(4): p. 521-523.  
9 504 9. Schmeisser, D., R.D. Schnell, A. Bogen, F.J. Himpsel, D. Rieger, G.  
10 505 Landgren, and J.F. Morar, *Surface Oxidation States of Germanium.*  
11 506 *Surface Science*, 1986. **172**(2): p. 455-465.  
12 507 10. Binder, J.F., P. Broqvist, and A. Pasquarello, *Charge Trapping in*  
13 508 *Substoichiometric Germanium Oxide.* *Microelectronic Engineering*,  
14 509 2011. **88**(7): p. 1428-1431.  
15 510 11. Bodlaki, D., H. Yamamoto, D.H. Waldeck, and E. Borguet, *Ambient*  
16 511 *Stability of Chemically Passivated Germanium Interfaces.* *Surface*  
17 512 *Science*, 2003. **543**(1): p. 63-74.  
18 513 12. Loscutoff, P.W. and S.F. Bent, *Reactivity of the Germanium Surface:*  
19 514 *Chemical Passivation and Functionalization.* *Annual Review of*  
20 515 *Physical Chemistry*, 2006. **57**: p. 467-495.  
21 516 13. Ardalan, P., Y. Sun, P. Pianetta, C.B. Musgrave, and S.F. Bent,  
22 517 *Reaction Mechanism, Bonding, and Thermal Stability of 1-*  
23 518 *Alkanethiols Self-Assembled on Halogenated Ge Surfaces.* *Langmuir*,  
24 519 2010. **26**(11): p. 8419-8429.  
25 520 14. Cullen, G.W., J.A. Amick, and D. Gerlich, *The Stabilization of*  
26 521 *Germanium Surfaces by Ethylation.* *Journal of The Electrochemical*  
27 522 *Society*, 1962. **109**(2): p. 124-127.  
28 523 15. Choi, K. and J.M. Buriak, *Hydrogermylation of Alkenes and Alkynes*  
29 524 *on Hydride-Terminated Ge(100) Surfaces.* *Langmuir*, 2000. **16**(20):  
30 525 p. 7737-7741.  
31 526 16. Hanrath, T. and B.A. Korgel, *Chemical Surface Passivation of Ge*  
32 527 *Nanowires.* *Journal of the American Chemical Society*, 2004.  
33 528 **126**(47): p. 15466-15472.  
34 529 17. Han, S.M., W.R. Ashurst, C. Carraro, and R. Maboudian, *Formation*  
35 530 *of Alkanethiol Monolayer on Ge(111).* *Journal of the American*  
36 531 *Chemical Society*, 2001. **123**(10): p. 2422-2425.  
37  
38  
39  
40  
41  
42  
43  
44  
45  
46  
47  
48

- 1  
2  
3 532 18. Bachelet, G.B. and M. Schlüter, *Structural Determination of Cl*  
4 533 *Chemisorption on Si{111} and Ge{111} by Total-Energy*  
5 534 *Minimization*. Physical Review B, 1983. **28**(4): p. 2302-2304.  
6  
7 535 19. Citrin, P.H., J.E. Rowe, and P. Eisenberger, *Direct Structural Study*  
8 536 *of Cl on Si {111} and Ge {111} Surfaces: New Conclusions*. Physical  
9 537 Review B, 1983. **28**(4): p. 2299-2301.  
10 538 20. Fouchier, M., M.T. McEllistrem, and J.J. Boland, *Novel Adatom-*  
11 539 *Terminated Step Structure on the Ge(111)-(1×1):Br Surface*. Surface  
12 540 Science, 1997. **385**(1): p. 1905-1910.  
13 541 21. Göthelid, M., G. LeLay, C. Wigren, M. Björkqvist, and U.O.  
14 542 Karlsson, *Iodine Reaction and Passivation of the Ge(111) Surface*.  
15 543 Surface Science, 1997. **371**(2): p. 264-276.  
16 544 22. Dharma-wardana, M.W.C., M.Z. Zgierski, D. Ritchie, J.G. Ping, and  
17 545 H. Ruda, *Comparison of Cluster and Slab Models of the Surface*  
18 546 *Structure of Cl-Terminated Ge(111) and GaAs(111) Surfaces*.  
19 547 Physical Review B, 1999. **59**(24): p. 15766-15771.  
20 548 23. Cao, S., J.C. Tang, and S.L. Shen, *Multiple-Scattering and DV-Xa*  
21 549 *Analyses of a Cl-Passivated Ge(111) Surface*. Journal of Physics:  
22 550 Condensed Matter, 2003. **15**(30): p. 5261-5268.  
23 551 24. Lal, P., A.V. Teplyakov, Y. Noah, M.J. Kong, G.T. Wang, and S.F.  
24 552 Bent, *Adsorption of Ethylene on the Ge(100)-2×1 Surface: Coverage*  
25 553 *and Time-Dependent Behavior*. The Journal of Chemical Physics,  
26 554 1999. **110**(21): p. 10545-10553.  
27 555 25. Teplyakov, A.V., P. Lal, Y.A. Noah, and S.F. Bent, *Evidence for a*  
28 556 *Retro-Diels–Alder Reaction on a Single Crystalline Surface:*  
29 557 *Butadienes on Ge(100)*. Journal of the American Chemical Society,  
30 558 1998. **120**(29): p. 7377-7378.  
31 559 26. Lee, S.W., J.S. Hovis, S.K. Coulter, R.J. Hamers, and C.M. Greenlief,  
32 560 *Cycloaddition Chemistry on Germanium(001) Surfaces: the*  
33 561 *Adsorption and Reaction of Cyclopentene and Cyclohexene*. Surface  
34 562 Science, 2000. **462**(1): p. 6-18.  
35 563 27. Filler, M.A., J.A. Van Deventer, A.J. Keung, and S.F. Bent,  
36 564 *Carboxylic Acid Chemistry at the Ge(100)-2 × 1 Interface: Bidentate*

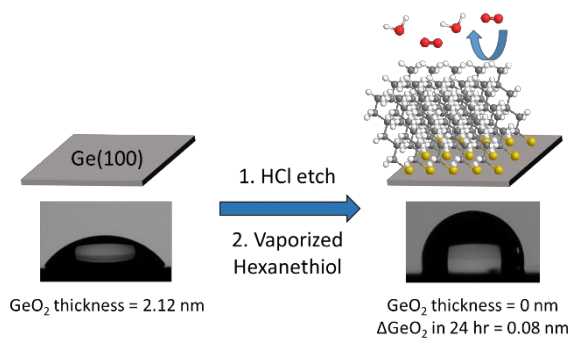
- 1  
2  
3 565 *Bridging Structure Formation on a Semiconductor Surface*. Journal  
4 566 of the American Chemical Society, 2006. **128**(3): p. 770-779.
- 5 567 28. Ardalan, P., N. Davani, and C.B. Musgrave, *Attachment of Alanine*  
6 568 *and Arginine to the Ge(100)-2×1 Surface*. The Journal of Physical  
7 569 Chemistry C, 2007. **111**(9): p. 3692-3699.
- 8 570 29. Ardalan, P., C.B. Musgrave, and S.F. Bent, *Formation of*  
9 571 *Alkanethiolate Self-Assembled Monolayers at Halide-Terminated Ge*  
10 572 *Surfaces*. Langmuir, 2009. **25**(4): p. 2013-2025.
- 11 573 30. Paine, D.C., J.J. Rosenberg, S.C. Martin, D. Luo, and M. Kawasaki,  
12 574 *Evaluation of Device Quality Germanium-Germanium Oxynitride*  
13 575 *Interfaces by High-Resolution Transmission Electron Microscopy*.  
14 576 Applied Physics Letters, 1990. **57**(14): p. 1443-1445.
- 15 577 31. Tindall, C. and J.C. Hemminger, *HREELS Studies of the Chemistry*  
16 578 *of Nitrogen Hydrides on Ge(100): Formation of a Surface Nitride at*  
17 579 *Low Temperatures*. Surface Science, 1995. **330**(1): p. 67-74.
- 18 580 32. Kim, H., P.C. McIntyre, C.O. Chui, K.C. Saraswat, and M.-H. Cho,  
19 581 *Interfacial Characteristics of HfO<sub>2</sub> Grown on Nitrated Ge (100)*  
20 582 *Substrates by Atomic-Layer Deposition*. Applied Physics Letters,  
21 583 2004. **85**(14): p. 2902-2904.
- 22 584 33. Maggioni, G., S. Carturan, L. Fiorese, N. Pinto, F. Caproli, D.R.  
23 585 Napoli, M. Giarola, and G. Mariotto, *Germanium Nitride and*  
24 586 *Oxynitride Films for Surface Passivation of Ge Radiation Detectors*.  
25 587 Applied Surface Science, 2017. **393**: p. 119-126.
- 26 588 34. Tao, Y., R. Hauert, and C.L. Degen, *Exclusively Gas-Phase*  
27 589 *Passivation of Native Oxide-Free Silicon(100) and Silicon(111)*  
28 590 *Surfaces*. ACS Applied Materials & Interfaces, 2016. **8**(20): p.  
29 591 13157-13165.
- 30 592 35. Kosuri, M.R., H. Gerung, Q.M. Li, S.M. Han, B.C. Bunker, and T.M.  
31 593 Mayer, *Vapor-Phase Adsorption Kinetics of 1-Decene on H-*  
32 594 *Terminated Si(100)*. Langmuir, 2003. **19**(22): p. 9315-9320.
- 33 595 36. Kosuri, M., H. Gerung, Q. li, S. Han, P. Herrera-Morales, and J.  
34 596 Weaver, *Vapor-Phase Adsorption Kinetics of 1-Decene on*  
35 597 *Hydrogenated Si(111)*. Surface Science, 2005. **596**: p. 21-38.
- 36  
37  
38  
39  
40  
41  
42  
43  
44  
45  
46  
47  
48

- 1  
2  
3 598 37. Kosuri, M.R., R. Cone, Q. Li, S.M. Han, B.C. Bunker, and T.M.  
4 599 Mayer, *Adsorption Kinetics of 1-Alkanethiols on Hydrogenated*  
5 600 *Ge(111)*. *Langmuir*, 2004. **20**(3): p. 835-840.  
6 601 38. Takenaka, M., K. Morii, M. Sugiyama, Y. Nakano, and S. Takagi,  
7 602 *Gas Phase Doping of Arsenic into (100), (110), and (111)*  
8 603 *Germanium Substrates Using a Metal–Organic Source*. *Japanese*  
9 604 *Journal of Applied Physics*, 2011. **50**: p. 010105.  
10 605 39. Takenaka, M., K. Morii, M. Sugiyama, Y. Nakano, and S. Takagi,  
11 606 *Dark Current Reduction of Ge Photodetector by GeO<sub>2</sub> Surface*  
12 607 *Passivation and Gas-Phase Doping*. *Optics Express*, 2012. **20**(8): p.  
13 608 8718-8725.  
14 609 40. *International Roadmap for Devices and Systems, in More Moore*.  
15 610 2018.  
16 611 41. Tao, Y., P. Navaretti, R. Hauert, U. Grob, M. Poggio, and C.L. Degen,  
17 612 *Permanent Reduction of Dissipation in Nanomechanical Si*  
18 613 *Resonators by Chemical Surface Protection*. *Nanotechnology*, 2015.  
19 614 **26**(46): p. 465501.  
20 615 42. Cai, Q., B. Xu, L. Ye, Z. Di, S. Huang, X. Du, J. Zhang, Q. Jin, and  
21 616 J. Zhao, *1-Dodecanethiol Based Highly Stable Self-Assembled*  
22 617 *Monolayers for Germanium Passivation*. *Applied Surface Science*,  
23 618 2015. **353**: p. 890-901.  
24 619 43. Collins, G., D. Aureau, J.D. Holmes, A. Etcheberry, and C. O'Dwyer,  
25 620 *Germanium Oxide Removal by Citric Acid and Thiol Passivation*  
26 621 *from Citric Acid-Terminated Ge(100)*. *Langmuir*, 2014. **30**(47): p.  
27 622 14123-14127.  
28 623 44. Graupe, M., T. Koini, H.I. Kim, N. Garg, Y.F. Miura, M. Takenaga,  
29 624 S.S. Perry, and T.R. Lee, *Self-Assembled Monolayers of CF<sub>3</sub>-*  
30 625 *Terminated Alkanethiols on Gold*. *Colloids and Surfaces A:*  
31 626 *Physicochemical and Engineering Aspects*, 1999. **154**(1): p. 239-244.  
32 627 45. Vericat, C., M.E. Vela, G. Benitez, P. Carro, and R.C. Salvarezza,  
33 628 *Self-Assembled Monolayers of Thiols and Dithiols on Gold: New*  
34 629 *Challenges for a Well-Known System*. *Chemical Society Reviews*,  
35 630 2010. **39**(5): p. 1805-1834.  
36  
37  
38  
39  
40  
41  
42  
43  
44  
45  
46  
47  
48

- 1  
2  
3 631 46. Bhartia, B., S.R. Puniredd, S. Jayaraman, C. Gandhimathi, M.  
4 632 Sharma, Y.-C. Kuo, C.-H. Chen, V.J. Reddy, C. Troadec, and M.P.  
5 633 Srinivasan, *Highly Stable Bonding of Thiol Monolayers to Hydrogen-*  
6 634 *Terminated Si via Supercritical Carbon Dioxide: Toward a Super*  
7 635 *Hydrophobic and Bioresistant Surface*. ACS Applied Materials &  
8 636 Interfaces, 2016. **8**(37): p. 24933-24945.
- 10 637 47. Laibinis, P.E. and G.M. Whitesides, *Self-Assembled Monolayers of*  
11 638 *n-Alkanethiolates on Copper are Barrier Films that Protect the Metal*  
12 639 *Against Oxidation by Air*. Journal of the American Chemical Society,  
13 640 1992. **114**(23): p. 9022-9028.
- 15 641 48. Bal, J., S. Kundu, and S. Hazra, *Hydrophilic-Like Wettability of Cl-*  
16 642 *Passivated Ge(001) Surface*. Chemical Physics, 2012. **406**: p. 72.
- 17 643 49. van Dorp, D.H., D. Weinberger, S. Van Wonterghem, S. Arnauts, K.  
18 644 Strubbe, F. Holsteyns, and S. De Gendt, *Nanoscale Etching:*  
19 645 *Dissolution of III-As and Ge in HCl/H2O2 Solutions*. ECS  
20 646 Transactions, 2015. **69**(8): p. 235-242.
- 22 647 50. Hohman, J.N., M. Kim, H.R. Bednar, J.A. Lawrence, P.D.  
23 648 McClanahan, and P.S. Weiss, *Simple, Robust Molecular Self-*  
24 649 *Assembly on Germanium*. Chemical Science, 2011. **2**(7): p. 1334-  
25 650 1343.
- 26 651 51. Murakami, H., T. Fujioka, A. Ohta, T. Bando, S. Higashi, and S.  
27 652 Miyazaki, *Characterization of Interfaces between Chemically*  
28 653 *Cleaned or Thermally Oxidized Germanium and Metals*. 2010, ECS.
- 30 654 52. Deegan, T. and G. Hughes, *An X-Ray Photoelectron Spectroscopy*  
31 655 *Study of the HF Etching of Native Oxides on Ge(111) and Ge(100)*  
32 656 *Surfaces*. Applied Surface Science, 1998. **123-124**: p. 66-70.
- 33 657 53. Cumpson, P.J., *The Thickogram: a Method for Easy Film Thickness*  
34 658 *Measurement in XPS*. Surface and Interface Analysis, 2000. **29**(6): p.  
35 659 403-406.

37 660

40 661

662 **Table of Contents Graphic**

663

664

665